Seasonal patterns of pig management in the Neolithic middle Yellow River region: evidence from carbon and oxygen isotopes in sequentially sampled tooth enamel

Quan Zhang[1,2,3], Yanfeng Hou[4*], Xinwei Li[5], Yu Dong[1,2], Amy Styring[3], Julia Lee-Thorp[3], Xiaolin Ma[6*]

1. Key Laboratory of Archaeological Sciences and Technology (Shandong University, Qingdao), Ministry of Education, China.
2. Institute of Cultural Heritage, Shandong University, Qingdao, China.
3. School of Archaeology, University of Oxford, Oxford, UK.
4. Henan Provincial Institute of Cultural Heritage and Archaeology, Zhengzhou, China.
5. Chinese Academy of History, Chinese Academy of Social Sciences, Beijing, China.
6. School of Cultural Heritage and Information Management, Shanghai University, Shanghai, China.

*Corresponding authors:
Yanfeng Hou, houyanfeng@126.com
Xiaolin Ma, xiaolinma@vip.163.com

Abstract

Domestic pigs became the primary source of meat in northern China by *ca* 6,000 cal yr B.P., coinciding with the intensification of C_4 millet agriculture. The seasonal

management of pig husbandry and its relationship with millet production, however, remain unclear. To explore the seasonal birthing, feeding, and drinking behaviours of Neolithic pigs, we analysed sequential tooth enamel oxygen ($\delta^{18}O$) and carbon ($\delta^{13}C$) isotope profiles of pigs from the site of Xipo (*ca* 5,800–5,000 cal yr B.P.), and compared them against those of modern wild boar. In contrast to the single birthing season (spring) for wild boar, the $\delta^{18}O$ profiles of Xipo pigs support the hypothesis of two birthing seasons, spring and autumn. These results provide some of the earliest evidence for off-season birthing in Neolithic pigs, suggesting an extension of the pig breeding season under human management. Also, in contrast to the low $\delta^{13}C$ values of wild C_3-foraging boar, the consistently high $\delta^{13}C$ values of Xipo pigs suggest year-round consumption of C_4 resources, most likely derived from millet by-products and other C_4 resources associated with settlement life. These findings suggest that Neolithic farmers in the middle Yellow River region managed the seasonality of pig breeding and feeding by *ca* 5,500 cal yr B.P. By this point, pig husbandry and millet farming had been integrated into a seasonal agricultural cycle.

Keywords: pig husbandry, millet farming, agricultural intensification, $\delta^{18}O$ and $\delta^{13}C$ profiles, birthing seasons, Northern China

1. Introduction

The domestication of the pig (*Sus scrofa*) marked a key milestone in the Neolithisation process in China, which profoundly reshaped human subsistence patterns (Dong and Yuan, 2020; Han et al., 2025). Following its initial domestication around 8,500 cal yr B.P. (Cucchi et al., 2011; Luo and Zhang, 2008), pig husbandry became increasingly important in the subsistence economy, eventually providing the predominant source of meat (50–80%) for Neolithic farmers in most regions of northern China by 6,000 cal yr B.P. (Luo, 2012). During 6,000 to 5,000 cal yr B.P.,

stable carbon and nitrogen isotope analyses of pig bone collagen indicate that pig diets shifted from C_3-dominated or C_3/C_4 mixed to C_4-dominated foods in the middle Yellow River region (e.g., Chen et al., 2016; Pechenkina et al., 2005). Both cultivated foxtail millet (*Setaria italica*) and broomcorn millet (*Panicum miliaceum*) follow the C_4 photosynthesis pathway, whereas the natural vegetation in this region is predominantly C_3 plants. Thus, this dietary shift has been widely interpreted as increased reliance on millet-derived resources in pig diets (Barton et al., 2009). It also suggests a transition from extensive management, likely involving free foraging in natural C_3 ecosystems, to tighter human control over both pig diet and movement, characterised by millet-based feeding and more restricted ranging or penning (Yang et al., 2022; Zhang et al., 2021). The substantial labour inputs involved in such a crop-based feeding strategy point strongly to a marked intensification of pig husbandry, defined here as increased investment of labour, time, and management in animal production to enhance productivity and reliability. However, seasonal pig management strategies during this transition remain poorly understood. Given that millets were harvested in early autumn, how did the pig feeding practices vary seasonally to regulate the intra-annual fluctuations in food resources? Mortality profiles indicate that most pigs were slaughtered at one to two years of age, when they reached their highest feed-to-yield efficiency (Ma, 2007a), raising the question of whether pigs' birth seasons extended to maintain a year-round pork supply. More broadly, how did the seasonal feeding practices coordinate with the growth cycle of millets and the birthing seasons of pigs within the annual farming calendar?

Reproduction is known to be seasonal in wild boar (Mauget, 1982). Sows typically farrow once a year in late spring, thus giving their offspring the best chances of survival. Natural photoperiod plays an important role in controlling melatonin synthesis and, in turn, seasonal breeding in wild boar (Malpaux et al., 1999). In contrast, modern domestic pigs can reproduce all year round under favourable

conditions. When and how this transition from seasonal to year-round reproduction occurred during the domestication process remains poorly understood. Previous studies have examined linear enamel hypoplasia (LEH) to infer pig birthing seasons in Neolithic China, suggesting single spring farrowing for pigs dated to *ca* 7,000–5,500 cal yr B.P. in the Wei River valley (Wang et al., 2012), and possible double farrowing from *ca* 5,500–5,000 cal yr B.P. at the Longshangang site in the upper Hanjiang River valley (Pike-Tay et al., 2016). However, LEH records only episodes of physiological stress and does not allow for a detailed reconstruction of seasonal activities.

Sequential tooth enamel oxygen ($\delta^{18}O$) and carbon ($\delta^{13}C$) isotope profiles are powerful tools for indicating seasonal activities in animals' early life (Pederzani and Britton, 2019). Enamel bioapatite $\delta^{13}C$ values reflect the integration of isotopic compositions of all dietary carbon (Ambrose and Norr, 1993; Lee-Thorp et al., 1989; Passey et al., 2005), so variation in intra-tooth sequential $\delta^{13}C$ values of *Sus* (domestic pigs and/or wild boar) can reflect shifts in their dietary carbon sources, thereby offering seasonal insights into pig feeding or foraging. Enamel bioapatite $\delta^{18}O$ values closely reflect those of ingested water through drinking and eating (Kirsanow and Tuross, 2011; Luz et al., 1984; Podlesak et al., 2008), which normally track $\delta^{18}O$ values of local meteoric water (Cernusak et al., 2016). Thus, intra-tooth sequential $\delta^{18}O$ values may be used to indicate the seasonality of *Sus* water intake with reference to the seasonal $\delta^{18}O$ variation in local meteoric water. We therefore hypothesised that pigs born in different seasons would exhibit distinct patterns in their tooth enamel $\delta^{18}O$ profiles and, if dietary carbon sources varied seasonally, correspondingly distinct $\delta^{13}C$ profiles. To test this hypothesis, we analysed sequential tooth enamel $\delta^{18}O$ and $\delta^{13}C$ profiles of both modern and archaeological *Sus* specimens from the middle Yellow River region of China, influenced by the East Asian monsoon (EAM).

Seasonal patterns in intra-tooth $\delta^{18}O$ profiles have been widely used to reconstruct animal birth seasonality, seasonal feeding practices, transhumance, and palaeoenvironments in temperate regions (e.g., Balasse et al., 2012; Blumenthal et al., 2019; Makarewicz, 2017; Tornero et al., 2020; Zazzo et al., 2010a), where $\delta^{18}O$ profiles typically exhibit a unimodal curve in a one-year cycle, with (dry) summer months showing higher $\delta^{18}O$ values than (wet) winter months. In contrast, seasonal $\delta^{18}O$ patterns for animals from the EAM region have been less studied. The EAM brings heavy summer rainfall, producing an 'amount effect' (Dansgaard, 1964; Rozanski et al., 1993) in which higher precipitation leads to lower $\delta^{18}O$ values in summer. A study on Late Neolithic–Bronze Age animals from the Central Plain, China, showed an annual bimodal pattern in tooth enamel $\delta^{18}O$ values in some cattle, attributed to the influence of the summer monsoon (Dai et al., 2016). Whether similar seasonal patterns occur in pigs under the EAM climate has not yet been investigated. Although sequential tooth enamel isotope analysis has been extensively applied to herbivores with high-crowned teeth, such as cattle, caprines, and horses, its application to omnivorous pigs remains limited, partly due to their bunodont molars with short crowns. Frémondeau *et al.* (2012) first demonstrated the feasibility of this method on non-molar teeth (incisors) of modern Corsican domestic and feral pigs to infer their birth seasonality, and subsequently identified multiple birthing seasons for pigs from an Iron Age settlement in France (Frémondeau et al., 2015) and Early Byzantine Sagalassos in Turkey (Frémondeau et al., 2017). The current isotopic studies on pig domestication and husbandry in Neolithic China have focused on bulk bone collagen isotope analyses, which preferentially reflect long-term dietary protein but lack intra-annual seasonal resolution. To our knowledge, this study provides the first seasonal-scale isotopic reconstruction of Neolithic pig husbandry practices in China using sequential tooth enamel isotope analysis.

Here, we analysed sequential $\delta^{18}O$ and $\delta^{13}C$ values in tooth enamel of *Sus* samples from the Xipo site (5,800–5,000 cal yr B.P.; Fig. 1), Henan province. To characterise the seasonal patterns of precipitation $\delta^{18}O$ values in this EAM-influenced region, we used monthly precipitation $\delta^{18}O$ data from Zhengzhou city (Fig. 1), Henan province, as a modern guide. We also measured intra-tooth sequential $\delta^{18}O$ and $\delta^{13}C$ values of modern wild boar inhabiting the natural woodland of the Wangwu Mountains (Fig. 1). This modern dataset reflects the natural patterns of $\delta^{18}O$ variations primarily driven by seasonal precipitation, $\delta^{13}C$ values of diets and seasonal dietary variation typical of woodland foraging, and provides isotopic evidence for determining the birth season of wild boar. By comparing the $\delta^{18}O$ and $\delta^{13}C$ profiles of Xipo *Sus* with those of the modern wild boar, we investigated how pig birthing seasons and seasonal diets differed under human management. This study aims to:

1. Establish seasonal patterns of tooth enamel $\delta^{18}O$ and $\delta^{13}C$ profiles for modern wild boar in the EAM-influenced region;
2. Reconstruct birth seasonality and seasonal dietary variation of Xipo *Sus* to infer seasonal Neolithic pig husbandry practices;
3. Evaluate how seasonal pig husbandry became integrated with the millet farming cycle during the Neolithic agricultural intensification process.

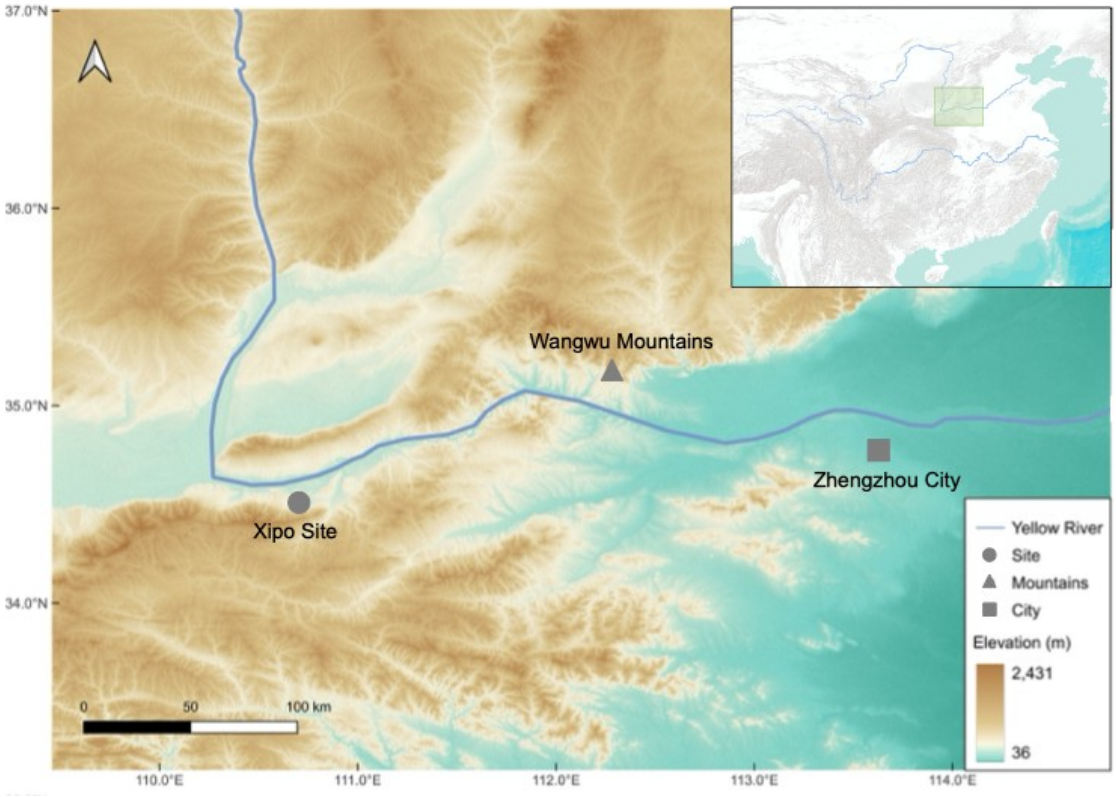

Fig. 1. Map of the Xipo site, Wangwu Mountains and Zhengzhou city. This map is made in QGIS 3.30 using Global Multi-resolution Terrain Elevation Data 2010 from USGS EROS (Danielson and Gesch, 2011).

2. Materials and Methods

2.1 Modern precipitation dataset

The Zhengzhou rainfall station (34.72N; 113.65E; 110 masl; Fig. 1) recorded monthly precipitation $\delta^{18}O$ values, amounts of precipitation, and air temperatures from 1985 to 1992 (Fig. 2a). This is the nearest station to Xipo (*ca* 270 km east) with available monthly precipitation $\delta^{18}O$ records. The two locations share similar latitude, precipitation regimes, and vapour sources under the EAM, making the Zhengzhou dataset the most appropriate modern reference for comparison. The sequence of precipitation $\delta^{18}O$ values follows an annual bimodal pattern (Fig. 2c). In summer, with the highest air temperatures and largest volumes of monsoonal rainfall, the 'amount

effect' is the dominant factor overwhelming the 'temperature effect', resulting in low precipitation $\delta^{18}O$ values (Qian et al., 2025). In winter, temperatures are lower and thus the fractionation effects become larger (Gat, 1996), leading to similarly low $\delta^{18}O$ values in cold months. Spring and autumn in between show relatively higher precipitation $\delta^{18}O$ values. The highest $\delta^{18}O$ values occur in April, when precipitation is low, and temperatures begin to rise. This EAM-influenced $\delta^{18}O$ pattern contrasts with that observed in most previously studied temperate climatic regions. As the timing of *Sus* tooth formation is predictable (Frémondeau et al., 2012), such seasonal patterns in precipitation $\delta^{18}O$ values offer a potential proxy for tracking the seasonality of *Sus* activities in the middle Yellow River region. We acknowledge that the Zhengzhou dataset serves as a modern analogue, used only to establish the seasonal patterns of $\delta^{18}O$ variations under EAM, rather than to infer absolute values.

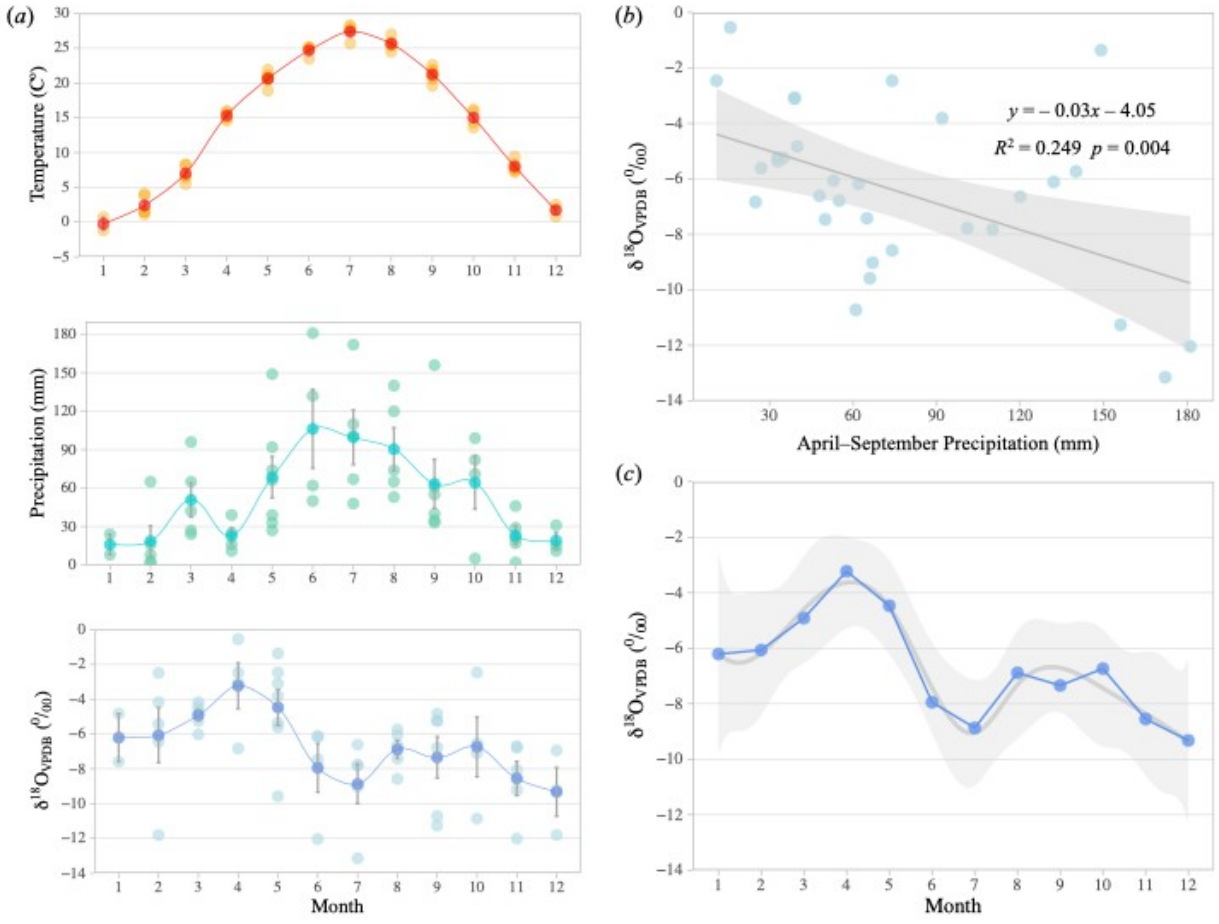

Fig. 2. (a) Monthly air temperatures, precipitation volumes and $\delta^{18}O$ values of precipitation at Zhengzhou from 1985 to 1992 (Data from the local Institute of Hydrogeology & Engineering Geology, Global Network of Isotopes in Precipitation programme, https://nucleus.iaea.org/wiser). Lighter-coloured circles represent the raw data; Darker-coloured circles represent the monthly mean values; Error bars represent the mean ±1 standard error; Splines are drawn interpolating the monthly means. (b) The correlation between precipitation $\delta^{18}O$ values and volumes from April to September. (c) The seasonal patterning of modern precipitation $\delta^{18}O$ values in one year at Zhengzhou. Spline (basis spline, degree = 8) and line are drawn interpolating the monthly means.

2.2 *Sus* specimens

Archaeological *Sus* samples were recovered from the Xipo site (34.50N; 110.71E; 456–475 masl; Fig. 1), a regional centre of the Middle Yangshao Culture in the middle Yellow River region (Li, 2013). This site is characterised by large communal buildings (> 200 m^2), rare well-decorated burials, and uneven distribution of exquisite burial objects among graves, suggesting increasing social complexity (Ma, 2005). Faunal remains, including pigs, recovered from the Xipo moat were directly dated to 5,600–5,000 cal yr B.P. (unpublished radiocarbon dates from the Xipo project, courtesy of Xinwei Li), corresponding to the peak occupation of the Xipo settlement. Zooarchaeological analyses indicate that most pigs were slaughtered before 1.5 years of age (Ma, 2007a). Their high bone collagen $\delta^{13}C$ values suggest that Xipo pigs were fed on C_4 resources and hence were intensively managed (Zhang et al., 2021).

Modern wild boar teeth were obtained from the Henan Provincial Institute of Cultural Heritage and Archaeology (Pike-Tay and Ma, 2013). These animals inhabited the Wangwu Mountains (34.88–35.27N; 112.03–112.75E; maximum elevation 1715.7 masl; Fig. 1), *ca* 150 km northwest of Xipo. The Wangwu Mountains are dominated

by natural temperate deciduous broadleaf and mixed coniferous-broadleaf woodlands, interspersed with shrublands and grasslands. Although these woodlands are relatively undisturbed, modern wild boar occasionally forage in surrounding farmland, particularly in maize, wheat, and sweet potato fields during the growing season.

2.3 Tooth enamel samples

As enamel is deposited incrementally from the apex to the cervix of the tooth crown and does not remodel after mineralisation, it provides a chronological isotopic archive of early life history. Enamel profiles represent essentially smoothed isotopic sequences, as the complex mineralisation during the prolonged stage of enamel maturation results in a time-averaging effect on isotopic compositions (Balasse, 2003; Green et al., 2017; Passey and Cerling, 2002; Zazzo et al., 2010), further complicated by the fact that multiple growth layers were sampled at once. This issue is more pronounced in *Sus* bunodont molars, which are unsuitable for sequential sampling. Therefore, *Sus* incisors (and, in some cases, canines) with higher crowns were used to obtain longer isotopic profiles. McCance *et al.* (1961) suggested that the crown of the lower first incisor (I_1) begins to form from the 2^{nd} to 3^{rd} month after birth, and that of the second incisor (I_2) formation starts from the 7^{th} month. Frémondeau *et al.* (2012) reported that I_1 records an isotopic archive from the 3^{rd} to 12^{th} month, while I_2 records from the 11^{th} to 19^{th} month for modern Corsican pigs born in November. Thus, I_1 is most appropriate for exploring the birthing season and early life history of *Sus*. Combined with I_2, it can extend isotopic records into sub-adulthood. Given the spring birth of wild boar in northern China, the estimated periods of I_1 and I_2 crown formation and the recorded periods in their isotopic profiles are illustrated in Fig. 3.

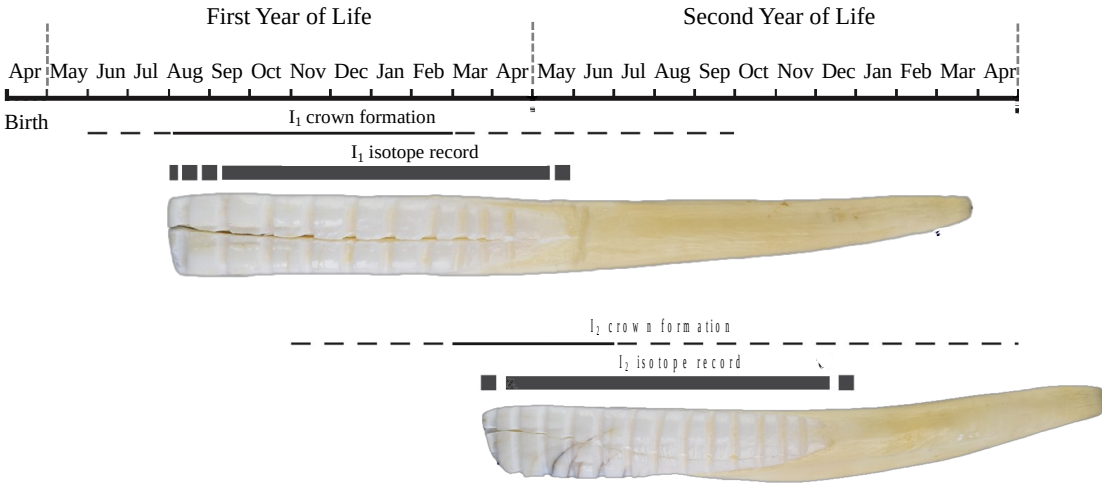

230

231 Fig. 3. Estimated periods of crown formation and those of sequential isotopic records
232 of I_1 and I_2 for *Sus* born in spring (April), after (Frémondeau et al., 2012). Lines
233 represent the reported timing of crown formation (McCance et al., 1961), with the
234 dotted parts showing variations; Bars represent the estimated timing of sequential
235 isotopic records (Frémondeau et al., 2012); Photographs show the sequentially
236 sampled I_1 and I_2 of the Henan modern wild boar in this study.
237
238 Intact I_1 and I_2 with little to no sign of wear were targeted for sequential sampling,
239 especially when both were available from the same individual. In total, eight I_1s and
240 four I_2s from modern wild boar were sequentially sampled. At Xipo, most *Sus* were
241 slaughtered at a young age when their I_2 formation had not yet started or completed
242 (Ma, 2007a). Thus, in most cases, only I_1 was available. Ten I_1s and only one
243 available I_2 (*Sus*-1) were sequentially sampled from Xipo. Enamel samples were
244 drilled in a series of 9 to 13 horizontal bands perpendicular to the growth axis of
245 incisors at regular intervals (Fig. 3). Sampling positions were recorded as distances
246 from the samples and the enamel-root junction (ERJ). Detailed sample information is
247 given in the Supplementary Material Table S1.

2.4 Preparation of enamel carbonate

Enamel samples were pre-treated using a modified dilute acetic acid (CH_3COOH) protocol (Sponheimer, 1999). Approximately 5 mg of powdered enamel sample was reacted with 1 ml 0.05 M CH_3COOH solution for 10 minutes at room temperature. Enamel samples were then rinsed three times with Milli-Q deionised water, centrifuged after each rinse, and oven-dried at 60°C. This mild pretreatment typically resulted in a mass loss exceeding 50%, consistent with previous studies (Snoeck and Pellegrini, 2015). Thus, to ensure sufficient material for isotope analysis, if a pre-treated sample was significantly less than 2 mg, it was combined with the next sample in the sequence to achieve the required mass.

2.5 Stable isotope analysis

Approximately 2 mg of enamel powder for each sample was weighed to determine the $^{18}O/^{16}O$ and $^{13}C/^{12}C$ ratios by mass spectrometry at the Stable Light Isotope Laboratory, Department of Archaeology, University of Cape Town, using a Thermo Delta V Advantage device equipped with a Gasbench. Stable carbon and oxygen isotope ratios are expressed using the delta (δ) notation as:

$$\delta^{18}O \text{ or } \delta^{13}C \ (‰) = \left(\frac{R_{sample} - R_{standard}}{R_{standard}} \right) \times 1000$$

where R = $^{18}O/^{16}O$ or $^{13}C/^{12}C$. The $\delta^{18}O$ and $\delta^{13}C$ values are both reported relative to the international Vienna PeeDee Belemnite (VPDB). Raw data in each run were calibrated against two international carbonate standards, Carrara-Marmor and IAEA-CO-8, (Gonfiantini et al., 1995) and two in-house powdered enamel standards from RLAHA, University of Oxford, Mammoth and Wildebeest (Supplementary Material Text S1). The standard deviations of measured $\delta^{13}C$ values for each sample determination ranged from 0.07‰ to 0.18‰, and those of $\delta^{18}O$ values ranged from 0.04‰ to 0.23‰. All the measurements are given in the Supplementary Material

Table S1. The proportions of C_4 and C_3 foods in *Sus* diets were estimated using a Bayesian stable isotope mixing model 'simmr' in R (Govan et al., 2023) (Supplementary Material Text S2).

3. Results

3.1 $\delta^{18}O$ and $\delta^{13}C$ values of the modern wild boar and Xipo *Sus*

The intra-tooth enamel carbonate $\delta^{18}O$ and $\delta^{13}C$ values of I_1s and I_2s for the Henan modern wild boar and Xipo *Sus* are summarised in Table 1, shown as boxplots in Fig. 4. The $\delta^{18}O$ values of the modern wild boar range widely from –10.0 to –2.7‰, with intra-tooth amplitudes of 1.1 to 7.3‰ (Table 1), comparable to the range of modern precipitation $\delta^{18}O$ values recorded at Zhengzhou (Fig. 2a). The $\delta^{18}O$ values of Xipo *Sus* range from –12.9 to –6.5‰, lower than those of both the modern wild boar and Zhengzhou precipitation, with minimal overlap. The $\delta^{13}C$ values of the modern wild boar range widely from –14.5 to –6.1‰, mostly clustering between –14 and –12‰ (Fig. 4a), suggesting a predominantly C_3 diet. In contrast, the $\delta^{13}C$ values of most Xipo *Sus* cluster from –3 to 0‰ (Fig. 4b), much higher than those of the modern wild boar. One individual (H6) shows distinctly lower $\delta^{13}C$ and higher $\delta^{18}O$ values than the other Xipo *Sus* (Supplementary Material Fig. S1), posited to be wild.

Table 1. Summary statistics of the I_1 and I_2 intra-tooth enamel $\delta^{18}O$ and $\delta^{13}C$ values for the Henan modern wild boar and Xipo *Sus*. Δ indicates the difference between the maxima and minima isotope values for each tooth.

Sample		ID	$\delta^{18}O$					$\delta^{13}C$					n
			Min	Max	$\Delta_{max-min}$	Mean	SD	Min	Max	$\Delta_{max-min}$	Mean	SD	
Modern	I_1	No.177	–10.0	–2.7	7.3	–4.9	2.1	–13.7	–9.2	4.5	–12.4	1.4	11
		No.188	–5.7	–3.2	2.5	–4.6	0.9	–13.9	–7.9	6	–12.3	1.9	10
		No.196	–6.4	–4.5	1.9	–5.3	0.7	–13.5	–12.3	1.2	–13.0	0.4	9
		No.216	–6.6	–5.5	1.1	–6.0	0.4	–14.5	–12.7	1.8	–13.7	0.6	11
		No.198	–7.5	–5.4	2.1	–6.6	0.5	–13.1	–11.6	1.5	–12.6	0.5	13

		No.182	–8.3	–5.8	2.5	–7.0	0.7	–14.2	–13.6	0.6	–13.9	0.2	10
		No.184	–8.7	–6.5	2.2	–7.4	0.7	–13.9	–12.9	1	–13.5	0.3	11
		No.171	–9.0	–6.1	2.9	–7.6	0.9	–13.5	–12.7	0.8	–13.3	0.3	9
	I_2	No.188	–9.8	–4.2	5.6	–7.1	2.2	–13.1	–6.1	7	–9.8	2.2	10
		No.196	–9.0	–5.7	3.3	–7.2	1.4	–13.8	–12.3	1.5	–13.0	0.5	10
		No.198	–9.5	–6.5	3	–8.0	1.0	–13.5	–10.4	3.1	–11.7	0.9	12
		No.171	–7.3	–6.2	1.1	–6.7	0.4	–13.5	–12.9	0.6	–13.2	0.2	10
Xipo	I_1	H6	–9.6	–6.5	3.1	–8.7	1.1	–10.2	–7.3	2.9	–9.3	0.9	7
		H5:22	–10.7	–8.7	2	–9.8	0.7	–4.5	–1.8	2.7	–2.8	0.9	9
		T315-3:20	–11.3	–9.6	1.7	–10.5	0.6	–1.6	–0.1	1.5	–0.7	0.4	9
		H115:5	–11.4	–9.3	2.1	–10.8	0.7	–1.2	0.3	1.5	–0.3	0.5	9
		H110:9	–12.1	–9.2	2.9	–10.8	0.7	–2.6	–0.7	1.9	–1.8	0.7	10
		H110:4	–11.7	–10.1	1.6	–11.0	0.7	–1.2	–0.2	1	–0.7	0.4	6
		H3-2:37	–11.8	–10.8	1	–11.3	0.3	–1.4	–0.4	1	–0.8	0.4	7
		H25:6	–12.0	–10.8	1.2	–11.4	0.4	–0.5	0.4	0.9	–0.2	0.3	10
		Sus1	–12.9	–9.8	3.1	–11.7	0.7	–2.7	–0.4	2.3	–1.5	0.9	11
		Sus2	–12.3	–10.5	1.8	–11.8	0.5	–1.5	–0.7	0.8	–1.2	0.2	9
	I_2	Sus1	–12.5	–10.7	1.8	–11.8	0.5	–3.7	–0.6	3.1	–1.5	0.9	12

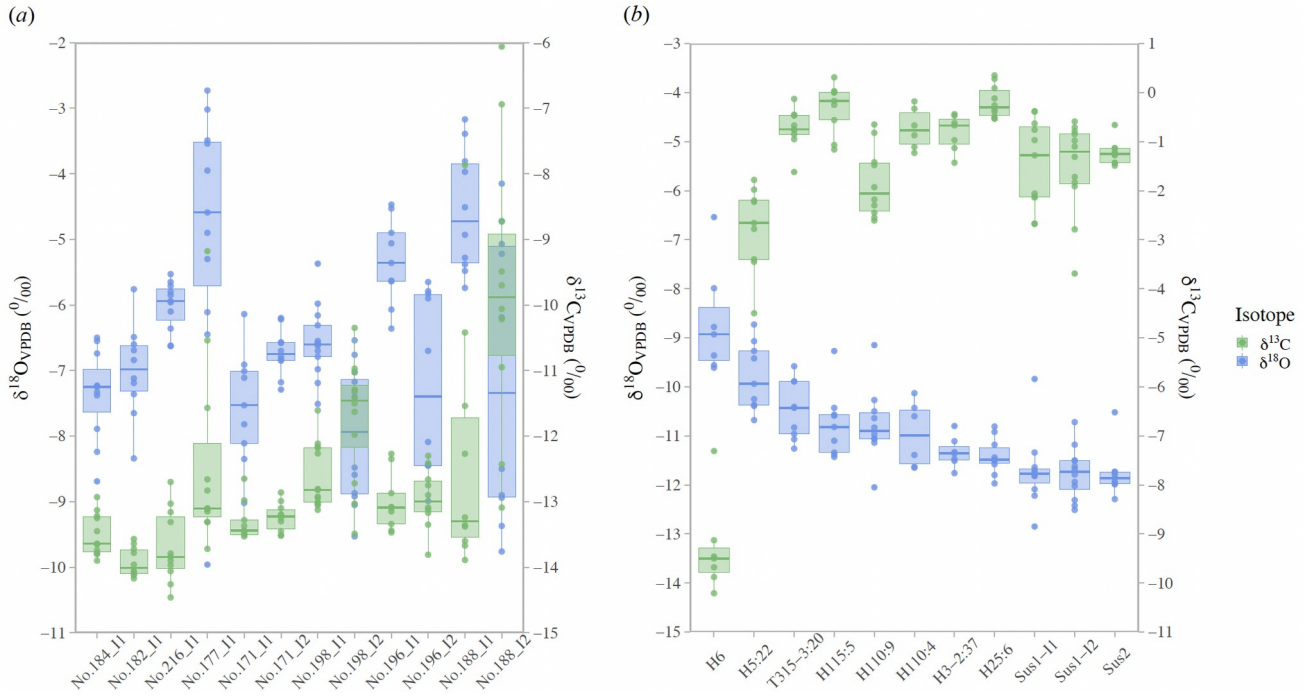

Fig. 4. Boxplots of $\delta^{18}O$ and $\delta^{13}C$ values for the Henan modern wild boar (a) and Xipo *Sus* (b).

3.2 $\delta^{18}O$ and $\delta^{13}C$ profiles of the modern wild boar and Xipo *Sus*

To investigate the birthing seasons of *Sus*, the intra-tooth sequential $\delta^{18}O$ and $\delta^{13}C$ values of I_1s from the modern wild boar and Xipo *Sus* are plotted against their sampled distances (Fig. 5a and b), with the tentatively wild individual H6 shown separately (Fig. 5c). As mentioned in Section 2.1, the seasonal pattern in precipitation $\delta^{18}O$ values under the EAM climate exhibits a bimodal curve in a one-year cycle (Fig. 2c). The enamel $\delta^{18}O$ profiles were therefore interpreted with reference to this seasonal precipitation $\delta^{18}O$ pattern rather than by fitting a sinusoidal model as previous studies did. To explore seasonal behaviours over a longer period by extending the lengths of isotopic profiles, the $\delta^{18}O$ and $\delta^{13}C$ profiles of paired I_1 and I_2 from four modern individuals and one archaeological individual, Xipo *Sus*-1, were graphically wiggle-matched on an individual basis (Fig. 6a and b), as crown length, growth rate, and duration of enamel formation vary among individuals. The $\delta^{18}O$ value of the final sample from I_1 of *Sus*-1 seems anomalously high and should be treated with caution, possibly because this enamel sample was not fully mineralised.

Fig. 5. The I_1 $\delta^{18}O$ and $\delta^{13}C$ values of sequential tooth enamel samples of Henan modern wild boar (a), Xipo *Sus* (b), and Xipo H6 (c). The seasonal patterning of modern precipitation $\delta^{18}O$ values at Zhengzhou and the estimated periods represented by the I_1s of the Henan modern wild boar that were born in spring (d) and those of Xipo *Sus* that were born in spring and autumn, respectively (e). The dashed line in (b) separates the two inferred birth seasons.

Fig. 6. The sequential tooth enamel $\delta^{18}O$ and $\delta^{13}C$ values of both I_1s and I_2s from four Henan modern wild boar (a) and Xipo *Sus*-1 (b). The seasonal patterning of modern precipitation $\delta^{18}O$ values at Zhengzhou and the estimated periods recorded by the I_1s and I_2s of the Henan modern wild boar (c) and Xipo *Sus*-1 (d). The grey bars below on each sub-plot display the sampled lengths of I_1s and I_2s, and where they are wiggle-matched. The zero point on the distance axis was set at the ERJ of I_1, with I_2 matched and aligned accordingly, thus some I_2 samples plotted at negative distances, following Frémondeau *et al.* (2012).

4. Discussion

4.1 Birth seasonality of the modern wild boar and Xipo *Sus*

For the modern wild boar, all their I_1 $\delta^{18}O$ profiles start with lower values and then tend to increase, although some fluctuations exist (Fig. 5a). This trend in increasing $\delta^{18}O$ values could correspond to either late summer to autumn (July to October) or late winter to spring (January to April), when compared to the annual bimodal pattern in Zhengzhou precipitation $\delta^{18}O$ profile (Fig. 2c). It is hard to distinguish between these two seasonal patterns based solely on $\delta^{18}O$ profiles. Thus, the changing trends in $\delta^{13}C$ profiles are also considered. Most I_1 $\delta^{13}C$ profiles are relatively flat with a slight rise approaching the end, while individuals No.177 and No.188 show marked increases in $\delta^{13}C$ values, suggesting more access to C_4 resources during the latter part of the isotopically recorded period (Fig. 5a). Since C_4 plants mostly grow in the warm season (Ehleringer et al., 1997), their consumption coincides with the final parts of the wild boar I_1 profiles. For individuals with both I_1 and I_2 data, the lowest $\delta^{18}O$ values (corresponding to July) often occur in their I_2 profiles (Fig. 6a). This suggests that their I_1 profiles likely end in early summer (June or May). Given that I_1 enamel records a period of *ca* 10 months, it is estimated that these I_1 profiles begin in late summer (Fig. 5d). As I_1 enamel formation starts from the 3rd month after birth, these modern wild boar are inferred to have been born in spring. The isotopic profiles of No.171 look slightly different from the others; however, the upward trend in its $\delta^{18}O$ profile resembles the early segments of others' profiles (Fig. 5a). Thus, this difference is more likely caused by its shorter incisors and, consequently, a shorter period recorded, rather than a different birthing season. This isotopic determination of spring birth for these wild boar is consistent with previous age estimates (Ma, 2010) and wildlife observations in the Wangwu Mountains (Wang et al., 2002). Overall, isotopic profiles of modern wild boar I_1s provide a sound estimation of birth season in this region.

Compared to the seasonal pattern of modern precipitation $\delta^{18}O$ profiles, the I_1 $\delta^{18}O$ profiles of Xipo *Sus* can be grouped into two distinct patterns, which are consistent with the hypothesis of two birthing seasons (Fig. 5e). Among the ten sampled Xipo individuals, seven (*Sus*-1, *Sus*-2, H115:5, H110:9, H25:6, T315-3:20, H6) show similar trends in I_1 $\delta^{18}O$ profiles. Their profiles begin with relatively low $\delta^{18}O$ values (inferred as summer), followed by a rise (autumn) and fall (winter), and finally rise to the highest values towards the end (spring). Considering the three-month interval between birth and the onset of I_1 formation, these individuals were most likely born in spring. However, their I_1 $\delta^{18}O$ profiles, including that of the tentatively wild *Sus* H6, differ from those of the modern wild boar also born in spring. This difference likely reflects that most Xipo *Sus* are estimated to have been born one to two months earlier than the modern wild boar (Fig. 5d and e). The $\delta^{13}C$ profile of *Sus* H6 differs from those of the managed pigs, with the highest $\delta^{13}C$ value occurring at the beginning of its I_1 profile (Fig. 5c), pointing to summer consumption of C_4 resources and again supporting its spring birth in the wild. Subtle variation in birthing time among individuals might make some look slightly different from others. Specifically, the I_1 of H110:9 likely formed earlier than that of T315-3:20, suggesting an earlier spring birth for the former. The remaining three individuals (H5:22, H110:4, H3-2:37) exhibit a different $\delta^{18}O$ pattern. Although their I_1 $\delta^{18}O$ profiles also begin with relatively low values, the highest values (most likely indicating spring) appear in the middle of the profiles instead of at the end, followed by a fall (summer) and rise (autumn) (Fig. 5b). Their I_1 crowns therefore likely began forming in early winter, indicating birth in early autumn. Their $\delta^{13}C$ profiles also show a similar shifting pattern, distinct from the other seven individuals (Fig. 5b). Taken together, the two patterns of sequential isotopic profiles for Xipo *Sus* support the hypothesis of two birthing seasons, interpreted here as spring and autumn. Compared with the single farrowing season of wild boar, the extended birthing seasons inferred for the Xipo pigs may have

increased sow productivity and potentially contributed to a more continuous pork supply. This management of reproductive seasonality represents a notable development in pig husbandry during the domestication process. The reconstructed seasonal patterns of birthing and feeding/foraging for Xipo *Sus* and modern wild boar are shown in Fig. 7.

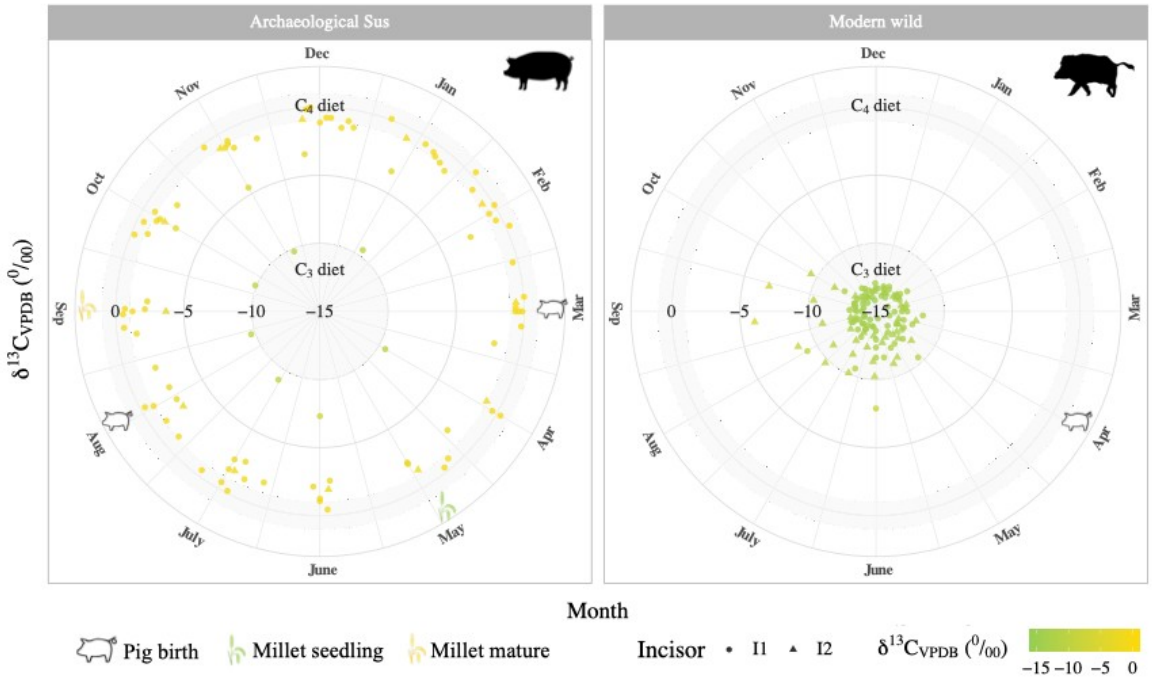

Fig. 7. Seasonal patterns of pig management at Xipo compared with those of modern wild foraging boar. The $\delta^{13}C$ values and seasonal patterns of birthing and feeding/foraging for archaeological *Sus* and modern wild boar were plotted as modelled annual cycles. The months corresponding to the $\delta^{13}C$ values were estimated from the sampling positions and the inferred start-end months of isotopic profiles. This timeline is approximate, due to the time-smoothing effect and the uneven growth rates in tooth enamel.

4.2 *Sus* seasonal diets and feeding practices

Enamel carbonate $\delta^{13}C$ values for the modern wild boar indicate that most individuals had predominantly C_3 diets, given that the averaged $\delta^{13}C$ difference between diet and

biomineral carbonate for *Sus* has been experimentally determined as +13.4‰ (Passey et al., 2005; Warinner and Tuross, 2009), and averaged $\delta^{13}C$ values for modern C_3 and C_4 plants are –27‰ and –12.5‰, respectively (Kohn, 2010; O'Leary, 1988). This result is consistent with open woodland foraging. Several individuals, however, show higher $\delta^{13}C$ values. No.188 I_2 records the highest $\delta^{13}C$ value of –6.1‰ among all the modern samples, suggesting an estimated dietary contribution of *ca* 54% C_4 resources (Supplementary Material Fig. S2). This peak occurs immediately after the lowest $\delta^{18}O$ value (normally July) in the profiles (Fig. 6a), corresponding to the late summer of its second year of life. Similar patterns are also observed for individuals No.177 and No.198 (Figs. 5a and 6a). Given the limited natural abundance of C_4 vegetation in the Wangwu Mountains, the higher $\delta^{13}C$ values likely reflect seasonal foraging on cultivated C_4 crops, probably maize, in surrounding farmland during the growing season.

Amongst the Xipo samples, *Sus* H6 is an outlier with the lowest mean $\delta^{13}C$ value of –9.3‰, indicating an estimated diet of *ca* 82% C_3 and 18% C_4 resources during I_1 formation (Supplementary Material Fig. S2). After correcting for the Suess effect (Indermühle et al., 1999) by subtracting 1.8‰, its $\delta^{13}C$ values fall within the range of the modern wild boar. Together with its distinct $\delta^{18}O$ profile, the isotopic pattern of *Sus* H6 is consistent with a hunted wild boar. In contrast, the relatively high enamel carbonate $\delta^{13}C$ values of the other Xipo pigs suggest that they had primarily C_4 diets during I_1 formation (Fig. 5b). The highest $\delta^{13}C$ value of +0.4‰ observed in H25:6 suggests *ca* 85% C_4 contribution to its diet (Supplementary Material Fig. S2). Given the dominance of millet cultivation in subsistence at Xipo, millet agricultural by-products, such as leaves and straw, are the most likely C_4 resources provided to Xipo pigs. Unlike the modern wild boar, in which elevated $\delta^{13}C$ values occur only during the C_4 growing season, Xipo pigs maintained high $\delta^{13}C$ values throughout the year (Fig. 5b). This pattern suggests that millet-derived resources were provided to

domestic pigs all year round, with the storage of millet by-products after the autumn harvest representing one possible management strategy. The entire annual cycle represented by *Sus*-1 profiles (Fig. 6b) further illustrates the seasonal feeding practices. Its $\delta^{13}C$ values increase after the first summer, remain high from autumn through winter, and then decrease from spring to summer of the next year. This seasonal dietary pattern suggests that millet-derived resources dominated pig diets throughout the year, with a notable increase after harvest, while the contribution of C_3 resources increased slightly during its second spring and summer. Individuals inferred to have been born in autumn display a different seasonal feeding pattern. Their higher $\delta^{13}C$ values appear in the middle of their I_1 profiles (Fig. 5b), corresponding to the lower $\delta^{18}O$ values (summer). Thus, they had greater C_4 consumption in their first summer, which is distinct from those born in spring. This difference may reflect age-specific husbandry practices, with both birth groups showing the greatest reliance on millet resources at around six months of age. This pattern may have resulted from interactions among weaning age, complementary feeding, juvenile nutritional requirements, and the seasonal availability of millet resources.

4.3 Whole diet vs dietary protein

To further investigate the specific sources of C_4 and C_3 resources, we compared the enamel carbonate $\delta^{13}C$ values with published bone collagen data for Xipo pigs (Zhang et al., 2021). Specifically, we assessed whether some C_4 inputs came from household waste, and whether C_3 resources were derived from human food scraps, C_3 plant fodder, or occasional foraging. Bioapatite CO_3 precipitates in equilibrium with blood bicarbonate, which is controlled by catabolic and respiratory processes and therefore reflects the whole diet, whereas collagen $\delta^{13}C$ values are strongly biased towards dietary protein (Ambrose and Norr, 1993; Lee-Thorp and van der Merwe, 1991). Thus, comparing enamel carbonate and bone collagen $\delta^{13}C$ values provides a means to distinguish whole-diet carbon sources from those derived predominantly from dietary

protein, offering additional insight into pig husbandry practices. In all cases, the estimated $\delta^{13}C$ values of long-term dietary protein sources are consistently higher than those of the entire diets during tooth formation (Supplementary Material Fig. S3). This suggests that dietary protein was predominantly from C_4 resources. Given the relatively low protein content of millet grains (*ca* 5–10%), they would not contribute much protein to pig diets. Possible protein-rich C_4 sources include household waste, such as scraps of C_4-fed pigs, and potentially human faeces. Human bone collagen samples from Xipo show a mean $\delta^{13}C$ value of –9.6 ± 1.0‰ (n = 30), consistent with substantial C_4 consumption (Zhang et al., 2011), and human faeces closely reflect dietary $\delta^{13}C$ values with a minor offset of –0.9‰ (Sponheimer et al., 2003). Moreover, archaeological evidence includes numerous miniature pottery sculptures of pigpens connected to latrines from the Han dynasty (202 BC–AD 220) (Supplementary Material Fig. S3), illustrating the connection between pig keeping and human waste recycling in historic China. A recent study further suggested that such practices could trace back to the early Neolithic, based on the presence of human whipworm eggs in pig dental calculus associated with exposure to human faecal material (Wang et al., 2025).

Conversely, the lower $\delta^{13}C$ values inferred for the whole diet relative to dietary protein suggest that the C_3 resources in pig diets had low protein content and thus were underrepresented in collagen $\delta^{13}C$ values. These C_3 resources were likely vegetation (e.g., vegetables, fruits, tubers) in natural and human-managed environments, since no evidence suggests substantial cultivation of C_3 cereal crops at Xipo (Zhong, 2016). Most pigs consumed more C_3 resources in spring and summer, when natural C_3 plants were growing, and the supply of stored C_4 resources would have been decreasing before the next millet harvest, although C_4 resources still dominated pig diets (> 50%). Taken together, these isotopic data indicate that in addition to year-round provisioning of millet by-products, human food waste and

faeces could also have been available to pigs, while C_3 vegetation contributed more in spring and summer before millet harvesting. Therefore, pigs were likely under close human management, with restricted ranging and regular feeding rather than being allowed to range freely. Such management would also have reduced crop damage during millet cultivation. Otherwise, as observed in the modern wild boar, C_3 resources would be expected to dominate pig diets except during the C_4 growing season.

4.4 Drinking water sources and seasonal activities

Given that the sampled modern wild boar are believed to have been born within a few years, the differences in their $\delta^{18}O$ values are unlikely to reflect long-term climatic change. Instead, they more likely reflect differences in drinking water sources and associated movement patterns, although interannual variations in precipitation and monsoon intensity may also have influenced. Based on the 'altitude effect', precipitation $\delta^{18}O$ values decrease with increasing altitude at –0.26‰/100 m (Poage and Chamberlain, 2001). The absolute height of the Wangwu Mountains is *ca* 1,300 m, which could potentially generate differences in precipitation $\delta^{18}O$ values up to approximately 3.4‰, providing a plausible explanation for $\delta^{18}O$ variation among individuals foraging and drinking at different elevations. Among the modern wild boar (Table 1), individuals No.177 and No.188 show the largest intra-tooth $\delta^{18}O$ variation (7.3‰ in No.177 I_1, n = 11; 5.6‰ in No.188 I_2, n = 10), and also the widest ranges of $\delta^{13}C$ values (7‰ in No.188 I_2, n = 10; 4.5‰ in No.177 I_1, n = 11). These individuals also display the highest $\delta^{13}C$ values among the modern samples, suggesting access to a broader spectrum of food resources, including seasonal consumption of C_4 resources, likely cultivated maize. The coincidence of large $\delta^{18}O$ and $\delta^{13}C$ variations indicates more extensive ranging behaviour, allowing access to diverse food and water sources across broader areas and elevations. However, the

potential influence of interannual variability in precipitation and monsoon activities cannot be ruled out.

The shifting patterns in $\delta^{18}O$ profiles of Xipo pigs closely follow the seasonal patterns in Zhengzhou precipitation $\delta^{18}O$ profiles (Figs. 5b and 6b), indicating that their drinking water sources tracked seasonal isotopic shifts in local precipitation. Thus, their drinking water likely came from small-bodied or temporary sources, such as ponds and moats found at Xipo, as well as nearby streams, which were fed primarily by local rainfall with short residence times (Koch et al., 1989). *Sus*-1 and *Sus*-2 show highly similar $\delta^{18}O$ and $\delta^{13}C$ profiles in their I_1s, suggesting comparable water sources and diets during their first year of life. These two pigs were found close to each other at the bottom of the moat, in similar postures with legs tied, likely buried at the same time. Given that both were inferred to have been born in spring within a few years, they may also have been managed similarly before this special burial. *Sus* H6, inferred as wild, shows $\delta^{18}O$ values *ca* 2‰ higher than those of the managed pigs (Table 1). This difference may reflect either the use of ^{18}O-enriched water sources when foraging in woodland, or greater intake of ^{18}O-enriched leaf water (Dongmann et al., 1974). However, precipitation and monsoon intensity vary interannually, and these individuals might have lived at different times. Thus, the observed inter-individual differences likely reflect a combination of ecological behaviours, environmental variability, and, potentially, differences in human management practices. Despite these uncertainties, the consistent seasonal patterns of enamel $\delta^{18}O$ profiles provide a robust framework for reconstructing seasonal husbandry practices at Xipo.

4.5 Shifts in monsoon intensity

Precipitation $\delta^{18}O$ values generally show a negative correlation with summer monsoon strength and rainfall amount across most of the EAM regions (Vuille et al., 2005). Thus, the significantly lower $\delta^{18}O$ values of Xipo *Sus* enamel compared to those of the

modern wild boar may reflect a more pronounced ‘amount effect’ associated with higher precipitation and intensified summer monsoon during the occupation of Xipo. However, *Sus* enamel $\delta^{18}O$ values are also influenced by drinking water sources, animal movement, human management, and interannual climatic variability, and thus cannot be interpreted as a direct proxy for local precipitation $\delta^{18}O$. Nevertheless, the lower $\delta^{18}O$ values of Xipo pigs are consistent with speleothem $\delta^{18}O$ records in China, which generally indicate enhanced summer monsoon during the mid-Holocene (Cai et al., 2010; Cosford et al., 2008; Dykoski et al., 2005). Additionally, abundant broad-leaved tree pollen and the frequent appearance of bamboo rats, water deer, water buffalo and freshwater molluscs in faunal assemblages together indicate a more humid climate between *ca* 6,000 and 5,000 cal yr B.P. (Chen et al., 2015; Lv and Zhang, 2008; Ma, 2007b). Although local meteoric water $\delta^{18}O$ values cannot be directly reconstructed from *Sus* enamel carbonate $\delta^{18}O$ values, multiple independent palaeoclimatic proxies collectively point to a wetter climate and enhanced monsoonal activity during this period.

5. Conclusions

Sequential tooth enamel $\delta^{18}O$ and $\delta^{13}C$ analyses provide seasonal-scale insights into *Sus* behaviours and Neolithic pig husbandry practices, including birth seasonality, drinking water sources, and feeding practices in the middle Yellow River region. The results support the hypothesis of two birthing seasons in Xipo pigs, interpreted as spring and autumn. This suggests an extension of the pig breeding season under intensive human management beyond the single spring farrowing typical of wild boar, which may have contributed to a more continuous pork supply throughout the year. The consistently higher $\delta^{13}C$ values of Xipo pigs compared with modern wild boar suggest that C_4 resources, most likely millet by-products such as leaves and straw, were fed to pigs all year round. Additionally, human food waste and/or faeces may also have contributed to pig diets, while more C_3 vegetation was consumed in spring

and summer before millet harvest. Our findings suggest that the management of pig reproductive seasonality had become part of pig husbandry practice in the middle Yellow River region by *ca* 5,500 cal yr B.P., representing a notable development during the process of pig domestication. By this point, pig husbandry practices and millet farming regimes had become integrated within a seasonal agricultural cycle. More broadly, this study highlights the potential of sequential enamel isotope analysis for reconstructing seasonal livestock management in the EAM region.

CRediT authorship contribution statement

Quan Zhang: Writing - Original Draft, Writing - Review & Editing, Conceptualisation, Methodology, Formal analysis, Visualisation, Software, Funding acquisition. **Yanfeng Hou:** Writing - Review & Editing, Conceptualisation, Investigation, Resources, Funding acquisition. **Xinwei Li:** Writing - Review & Editing, Project administration, Investigation, Resources. **Yu Dong:** Writing - Review & Editing, Project administration, Funding acquisition. **Amy Styring:** Writing - Review & Editing, Conceptualisation, Methodology, Supervision. **Julia Lee-Thorp:** Writing - Review & Editing, Conceptualisation, Methodology, Funding acquisition, Supervision. **Xiaolin Ma:** Writing - Review & Editing, Conceptualisation, Investigation, Resources, Project administration.

Funding

This project was funded by the National Key R&D Program of China (Grant NO. 2022YFF0903503), The Origin of Chinese Civilisation and Mount Songshan Civilisation Zhengzhou Research Association (Y2019-10), China Scholarship Council-University of Oxford Scholarship (CSC201604100068).

Declaration of competing interest

None.

Acknowledgements

We thank the Henan Provincial Institute of Cultural Heritage and Archaeology for permission to access the study materials and for providing us with continued support throughout the project. We are grateful to Dr. Peter Ditchfield and Dr. Julie Luyt for their laboratory assistance with the measurements of stable isotopes. We thank Dr. Qi Meng, Ms. Shufang Wang, Ms. Yujie Li, and Ms. Lulu He for their kind support with the sampling of faunal remains.

Appendix A. Supplementary data

Reference

Ambrose, S.H., Norr, L., 1993. Experimental evidence for the relationship of the carbon isotope ratios of whole diet and dietary protein to those of bone collagen and carbonate, in: Lambert, J.B., Grupe, G. (Eds.), Prehistoric Human Bone: Archaeology at the Molecular Level. Springer, pp. 1–37.

Balasse, M., 2003. Potential biases in sampling design and interpretation of intra-tooth isotope analysis. Int. J. Osteoarchaeol. 13, 3–10.

Balasse, M., Boury, L., Ughetto-Monfrin, J., Tresset, A., 2012. Stable isotope insights ($\delta^{18}O$, $\delta^{13}C$) into cattle and sheep husbandry at Bercy (Paris, France, 4th millennium BC): birth seasonality and winter leaf foddering. Environmental Archaeology 17, 29–44.

Barton, L., Newsome, S.D., Chen, F.-H., Wang, H., Guilderson, T.P., Bettinger, R.L., 2009. Agricultural origins and the isotopic identity of domestication in northern China. Proceedings of the National Academy of Sciences 106, 5523–5528.

Blumenthal, S.A., Cerling, T.E., Smiley, T.M., Badgley, C.E., Plummer, T.W., 2019. Isotopic records of climate seasonality in equid teeth. Geochim. Cosmochim. Acta 260, 329–348.

Cai, Y., Tan, L., Cheng, H., An, Z., Edwards, R.L., Kelly, M.J., Kong, X., Wang, X., 2010. The variation of summer monsoon precipitation in central China since the last deglaciation. Earth Planet. Sci. Lett. 291, 21–31.

Cernusak, L.A., Barbour, M.M., Arndt, S.K., Cheesman, A.W., English, N.B., Feild, T.S., Helliker, B.R., Holloway-Phillips, M.M., Holtum, J.A.M., Kahmen, A., 2016. Stable isotopes in leaf water of terrestrial plants. Plant Cell Environ. 39, 1087–1102.

Chen, F., Xu, Q., Chen, J., Birks, H.J.B., Liu, J., Zhang, S., Jin, L., An, C., Telford, R.J., Cao, X., 2015. East Asian summer monsoon precipitation variability since the last deglaciation. Sci. Rep. 5, 1–11.

Chen, X., Hu, S., Hu, Y., Wang, W., Ma, Y., Lü, P., Wang, C., 2016. Raising practices of Neolithic livestock evidenced by stable isotope analysis in the Wei River valley, North China. Int. J. Osteoarchaeol. 26, 42–52.

Dosford, J., Qing, H., Eglington, B., Mattey, D., Yuan, D., Zhang, M., Cheng, H., 2008. East Asian monsoon variability since the Mid-Holocene recorded in a high-resolution, absolute-dated aragonite speleothem from eastern China. Earth Planet. Sci. Lett. 275, 296–307.

Cucchi, T., Hulme-Beaman, A., Yuan, J., Dobney, K., 2011. Early Neolithic pig domestication at Jiahu, Henan Province, China: Clues from molar shape analyses using geometric morphometric approaches. J. Archaeol. Sci. 38, 11–22. https://doi.org/10.1016/j.jas.2010.07.024

Dai, L., Balasse, M., Yuan, J., Zhao, C., Hu, Y., Vigne, J.-D., 2016. Cattle and sheep raising and millet growing in the Longshan age in central China: Stable isotope investigation at the Xinzhai site. Quaternary International 426, 145–157.

Danielson, J.J., Gesch, D.B., 2011. Global multi-resolution terrain elevation data 2010 (GMTED2010): U.S. Geological Survey Open-File Report 2011–1073.

Dansgaard, W., 1964. Stable isotopes in precipitation. Tellus 16, 436–468.

Dong, N., Yuan, J., 2020. Rethinking pig domestication in China: regional trajectories in central China and the Lower Yangtze Valley. Antiquity 94, 864–879. https://doi.org/DOI: 10.15184/aqy.2020.122

Dongmann, G., Nürnberg, H.W., Förstel, H., Wagener, K., 1974. On the enrichment of $H_2{}^{18}O$ in the leaves of transpiring plants. Radiat. Environ. Biophys. 11, 41–52.

Dykoski, C.A., Edwards, R.L., Cheng, H., Yuan, D., Cai, Y., Zhang, M., Lin, Y., Qing, J., An, Z., Revenaugh, J., 2005. A high-resolution, absolute-dated Holocene and deglacial Asian monsoon record from Dongge Cave, China. Earth Planet. Sci. Lett. 233, 71–86.

Ehleringer, J.R., Cerling, T.E., Helliker, B.R., 1997. C_4 photosynthesis, atmospheric CO_2, and climate. Oecologia 112, 285–299.

Frémondeau, D., Cucchi, T., Casabianca, F., Ughetto-Monfrin, J., Horard-Herbin, M.-P., Balasse, M., 2012. Seasonality of birth and diet of pigs from stable isotope analyses of tooth enamel ($\delta^{18}O$, $\delta^{13}C$): a modern reference data set from Corsica, France. J. Archaeol. Sci. 39, 2023–2035.

Frémondeau, D., De Cupere, B., Evin, A., Van Neer, W., 2017. Diversity in pig husbandry from the Classical-Hellenistic to the Byzantine periods: An integrated dental analysis of Düzen Tepe and Sagalassos assemblages (Turkey). J. Archaeol. Sci. Rep. 11, 38–52.

Frémondeau, D., Horard-Herbin, M.-P., Buchsenschutz, O., Ughetto-Monfrin, J., Balasse, M., 2015. Standardized pork production at the Celtic village of Levroux Les Arènes

(France, 2nd c. BC): Evidence from kill-off patterns and birth seasonality inferred from enamel $\delta^{18}O$ analysis. J. Archaeol. Sci. Rep. 2, 215–226.

Gat, J.R., 1996. Oxygen and hydrogen isotopes in the hydrologic cycle. Annu. Rev. Earth Planet. Sci. 24, 225–262.

Govan, E., Jackson, A.L., Inger, R., Bearhop, S., Parnell, A.C., 2023. simmr: A package for fitting Stable Isotope Mixing Models in R. arXiv preprint arXiv:2306.07817.

Green, D.R., Green, G.M., Colman, A.S., Bidlack, F.B., Tafforeau, P., Smith, T.M., 2017. Synchrotron imaging and Markov Chain Monte Carlo reveal tooth mineralization patterns. PLoS One 12, e0186391.

Han, Y., Zhao, Z., Stanton, D.W.G., Lei, X.-L., Wu, Z., Liu, Y., Yu, C., Chen, X., Li, W., Wang, J., You, Y., Li, Y., Lei, S., Yi, H., Fan, W., Cai, Q., Min, R., Hu, C., Chen, C., Cui, Y., Guo, J., Zhang, H., Song, H., Guo, X., Ruan, Q., Tan, Y., Li, Z., Zhang, X., Shi, X., Zhou, X., Zhuang, Y., Manin, A., Frantz, L.A.F., Alves, J.M., Pan, Y., Wu, X., Luo, S.-J., Larson, G., Yu, H., 2025. Ancient Genomics Reveals the Origin, Dispersal, and Human Management of East Asian Domestic Pigs. Mol. Biol. Evol. 42, msaf214. https://doi.org/10.1093/molbev/msaf214

Indermühle, A., Stocker, T.F., Joos, F., Fischer, H., Smith, H.J., Wahlen, M., Deck, B., Mastroianni, D., Tschumi, J., Blunier, T., 1999. Holocene carbon-cycle dynamics based on CO 2 trapped in ice at Taylor Dome, Antarctica. Nature 398, 121–126.

Kirsanow, K., Tuross, N., 2011. Oxygen and hydrogen isotopes in rodent tissues: Impact of diet, water and ontogeny. Palaeogeogr. Palaeoclimatol. Palaeoecol. 310, 9–16.

Koch, P.L., Fisher, D.C., Dettman, D., 1989. Oxygen isotope variation in the tusks of extinct proboscideans: a measure of season of death and seasonality. Geology 17, 515–519.

Kohn, M.J., 2010. Carbon isotope compositions of terrestrial C_3 plants as indicators of (paleo)ecology and (paleo)climate. Proceedings of the National Academy of Sciences 107, 19691 LP – 19695. https://doi.org/10.1073/pnas.1004933107

Lee-Thorp, J.A., Sealy, J.C., Van Der Merwe, N.J., 1989. Stable carbon isotope ratio differences between bone collagen and bone apatite, and their relationship to diet. J. Archaeol. Sci. 16, 585–599.

Lee-Thorp, J.A., van der Merwe, N.J., 1991. Aspects of the chemistry of modern and fossil biological apatites. J. Archaeol. Sci. 18, 343–354.

Li, X., 2013. The Later Neolithic Period in the Central Yellow River Valley Area, c. 4000–3000 BC, in: Underhill, A.P. (Ed.), A Companion to Chinese Archaeology. Wiley-Blackwell, Oxford, pp. 213–235.

Luo, Y., 2012. The Domestication, Raising and Ritual Use of Pig in Ancient China. Science Press, Beijing (in Chinese).

Luo, Y., Zhang, J., 2008. Reanalyse the pig bones excavated from Jiahu site, Wuyang county, Henan province. Archaeology 90–96 (in Chinese).

Luz, B., Kolodny, Y., Horowitz, M., 1984. Fractionation of oxygen isotopes between mammalian bone-phosphate and environmental drinking water. Geochim. Cosmochim. Acta 48, 1689–1693.

Lv, H., Zhang, J., 2008. Neolithic cultural evolution and Holocene climate change in the Guanzhong Basin, Shaanxi, China. Quaternary Sciences 11.
Ma, X., 2010. A new perspective on the phenomenon of collective pig burials in ancient China: insights from modern wild boar studies, in: Zooarchaeology. Cultural Relics Press, Beijing, pp. 124–133 (in Chinese).
Ma, X., 2007a. Age composition of the domestic pigs of the Xipo site in Lingbao and related problems. Huaxia Archaeology 55–74 (in Chinese).
Ma, X., 2007b. Faunal remains from the Xipo site, Lingbao county, Henan province and related questions. Cultural Relics of Central China 48–61 (in Chinese).
Ma, X., 2005. Emergent Social Complexity in the Yangshao Culture: Analyses of Settlement Patterns and Faunal Remains from Lingbao, Western Henan, China c. 4900-3000 BC. British Archaeological Reports Limited.
Makarewicz, C.A., 2017. Sequential $\delta^{13}C$ and $\delta^{18}O$ analyses of early Holocene bovid tooth enamel: Resolving vertical transhumance in Neolithic domesticated sheep and goats. Palaeogeogr. Palaeoclimatol. Palaeoecol. 485, 16–29.
Malpaux, B., Thiéry, J.-C., Chemineau, P., 1999. Melatonin and the seasonal control of reproduction. Reprod. Nutr. Dev. 39, 355–366.
Mauget, R., 1982. Seasonality of reproduction in the wild boar. Control of pig reproduction 509–526.
McCance, R.A., Ford, E.H.R., Brown, W.A.B., 1961. Severe undernutrition in growing and adult animals: 7. Development of the skull, jaws and teeth in pigs. British Journal of Nutrition 15, 213–224.
O'Leary, M.H., 1988. Carbon isotopes in photosynthesis. Bioscience 38, 328–336.
Passey, B.H., Cerling, T.E., 2002. Tooth enamel mineralization in ungulates: implications for recovering a primary isotopic time-series. Geochim. Cosmochim. Acta 66, 3225–3234.
Passey, B.H., Robinson, T.F., Ayliffe, L.K., Cerling, T.E., Sponheimer, M., Dearing, M.D., Roeder, B.L., Ehleringer, J.R., 2005. Carbon isotope fractionation between diet, breath CO_2, and bioapatite in different mammals. J. Archaeol. Sci. 32, 1459–1470.
Pechenkina, E.A., Ambrose, S.H., Xiaolin, M., Benfer Jr, R.A., 2005. Reconstructing northern Chinese Neolithic subsistence practices by isotopic analysis. J. Archaeol. Sci. 32, 1176–1189.
Pederzani, S., Britton, K., 2019. Oxygen isotopes in bioarchaeology: Principles and applications, challenges and opportunities. Earth. Sci. Rev. 188, 77–107.
Pike-Tay, A., Ma, X., 2013. A pilot study in odontochronology for the pig domestication question in North-Central China. Int. J. Osteoarchaeol. 23, 590–599.
Pike-Tay, A., Ma, X., Hou, Y., Liang, F., Lin, M., Peterson, V., 2016. Combining odontochronology, tooth wear assessment, and linear enamel hypoplasia (LEH) recording to assess pig domestication in Neolithic Henan, China. Int. J. Osteoarchaeol. 26, 68–77.

Poage, M.A., Chamberlain, C.P., 2001. Empirical relationships between elevation and the stable isotope composition of precipitation and surface waters: considerations for studies of paleoelevation change. Am. J. Sci. 301, 1–15.
Podlesak, D.W., Torregrossa, A.-M., Ehleringer, J.R., Dearing, M.D., Passey, B.H., Cerling, T.E., 2008. Turnover of oxygen and hydrogen isotopes in the body water, CO2, hair, and enamel of a small mammal. Geochim. Cosmochim. Acta 72, 19–35.
Qian, Y., Wang, S., Zhang, M., Yoshimura, K., Bong, H., Yang, G., Li, H., 2025. Spatial pattern of amount effect of daily precipitation isotopes in China: A consideration of seasonality based on observation and simulation. J. Hydrol. (Amst). 653, 132793.
Rozanski, K., Araguás-Araguás, L., Gonfiantini, R., 1993. Isotopic patterns in modern global precipitation. GMS 78, 1–36.
Snoeck, C., Pellegrini, M., 2015. Comparing bioapatite carbonate pre-treatments for isotopic measurements: Part 1—Impact on structure and chemical composition. Chem. Geol. 417, 394–403.
Sponheimer, M., 1999. Isotopic Ecology of the Makapansgat Limeworks Fauna. Rutgers University.
Sponheimer, M., Robinson, T., Ayliffe, L., Passey, B., Roeder, B., Shipley, L., Lopez, E., Cerling, T., Dearing, D., Ehleringer, J., 2003. An experimental study of carbon-isotope fractionation between diet, hair, and feces of mammalian herbivores. Can. J. Zool. 81, 871–876.
Tornero, C., Balasse, M., Bréhard, S., Carrère, I., Fiorillo, D., Guilaine, J., Vigne, J.-D., Manen, C., 2020. Early evidence of sheep lambing de-seasoning in the Western Mediterranean in the sixth millennium BCE. Sci. Rep. 10, 1–11.
Vuille, M., Werner, M., Bradley, R.S., Keimig, F., 2005. Stable isotopes in precipitation in the Asian monsoon region. Journal of Geophysical Research: Atmospheres 110.
Wang, H., Martin, L., Hu, S., Wang, W., 2012. Pig domestication and husbandry practices in the middle Neolithic of the Wei River Valley, northwest China: evidence from linear enamel hypoplasia. J. Archaeol. Sci. 39, 3662–3670.
Wang, J., Li, S., Xia, W., Wang, W., Han, Q., Li, W., 2002. Biological characters and taming of wild pig. Journal of Economic Animal 6, 52–54.
Wang, J., Tang, Y., Zheng, Y., Jiang, L., Ma, X., Hou, Y., Sun, G., 2025. Early evidence for pig domestication (8,000 cal. BP) in the Lower Yangtze, South China. Proceedings of the National Academy of Sciences 122, e2507123122. https://doi.org/10.1073/pnas.2507123122
Warinner, C., Tuross, N., 2009. Alkaline cooking and stable isotope tissue-diet spacing in swine: archaeological implications. J. Archaeol. Sci. 36, 1690–1697.
Wang, J., Zhang, D., Yang, X., Wang, W., Perry, L., Fuller, D.Q., Li, H., Wang, J., Ren, L., Xia, H., 2022. Sustainable intensification of millet–pig agriculture in Neolithic North China. Nat. Sustain. 5, 780–786.
Zazzo, A., Balasse, M., Passey, B.H., Moloney, A.P., Monahan, F.J., Schmidt, O., 2010a. The isotope record of short-and long-term dietary changes in sheep tooth enamel:

implications for quantitative reconstruction of paleodiets. Geochim. Cosmochim. Acta 74, 3571–3586.

Zazzo, A., Balasse, M., Passey, B.H., Moloney, A.P., Monahan, F.J., Schmidt, O., 2010b. The isotope record of short-and long-term dietary changes in sheep tooth enamel: implications for quantitative reconstruction of paleodiets. Geochim. Cosmochim. Acta 74, 3571–3586.

Zhang, Q., Hou, Y., Li, X., Styring, A., Lee-Thorp, J., 2021. Stable isotopes reveal intensive pig husbandry practices in the middle Yellow River region by the Yangshao period (7000–5000 BP). PLoS One 16, e0257524.

Zhang, X., Zhao, X., Cheng, L., 2011. Human diets of Yangshao culture in the Central Plains. Chinese Archaeology 11, 188–196 (in Chinese).

Zhong, H., 2016. Paleoethnobotanic research on the Central Plain from the Middle-Yangshao to Longshan period. Ph.D. thesis. Graduate School of Chinese Academy of Social Sciences, Beijing, China (in Chinese).